

SPECIFICS OF ELECTRON DYNAMICS IN HIGH ENERGY CIRCULAR e+e- COLLIDERS*

Q. Qin[†], J. Gao, H.P. Geng, P. He, D. Wang, N. Wang, Y.W. Wang, Y. Zhang,
Institute of High Energy Physics, Chinese Academy of Sciences, Beijing, P.R. China

Abstract

As the demands of high energy physics, especially the newly found Higgs boson at the LHC, lepton circular collider looks much more promising than linear collider. But the energy will be 20% higher than the LEP operated about 20 years ago. Compare to the relative low energy electron circular collider, the high energy lepton collider has its special features, which influences the design of the whole machine and the beam dynamics. Specifics of beam dynamics, from linear lattice design to dynamics aperture, from beam-beam interaction to collective effects, will be discussed in this paper, together with the study of high energy circular collider CEPC and the FCC.

INTRODUCTION

The Higgs boson was declared to be discovered at the LHC 3 years ago with a mass of ~ 126 GeV/ c^2 , which is only about 20 GeV higher than the beam energy of LEP2. In Sept. 2012, two months later than the discovery of Higgs boson, IHEP announced a plan of building a circular electron positron collider (CEPC) as a Higgs factory in the next decade to study the features of Higgs, and some precise measurements on the Higgs particle. The CEPC can be converted to a super proton proton collider (SppC) in the same tunnel of CEPC. Meanwhile, TLEP, which was re-organized as FCC-hh, and $-ee$, were proposed by CERN as a future project after the LHC. In the following years, IHEP made some progresses on the pre-CDR study on the CEPC, including theory, machine and detector. In this paper, some specifics of the high energy electron positron collider will be discussed, and compared to the low energy e+e- collider like Beijing electron positron collider (BEPC).

BEAM-BEAM INTERACTION

In a circular e+e- collider, luminosity is determined by the beam-beam interaction to a great extent, which is often characterized as the so-called beam-beam parameter, ξ_y . In the design of the BEPC, the maximum design ξ_y is 0.04, and was achieved with optimizing other beam parameters in the luminosity tuning. At the large collider with high beam energy, the beam-beam parameter can be achieved as high as 0.08 or even 0.1[1]. In a round beam operation, ξ_y can even reach 0.15[2].

On the other hand, beam-beam interaction determines not only the luminosity, but the design, operation, and even the interaction region design of a collider. The colliding bunch current or the luminosity performance will be limited by this effect, which is called the beam-beam limit.

* Work supported by the innovation foundation of IHEP Y4545240Y2, 2015, and the National Foundation of Natural Sciences 11505198.

[†] qinq@ihep.ac.cn

The desire to achieve high luminosity leads one naturally to specify high currents and/or small beam sizes. These tend to make the beam-beam interaction stronger, which, in turn, may lead to beam blow-up, coherent oscillations, or fast particle losses that could defeat the purpose of the initial specification. The beam-beam parameter is defined as

$$\xi_{x,y} = \frac{r_e \beta_{x,y} N_b}{2\pi\gamma\sigma_{x,y}(\sigma_x + \sigma_y)}, \quad (1)$$

where γ denotes the relativistic Lorentz factor of the colliding particle, r_e the classical electron radius, N_b the bunch population of the each beam, $\beta_{x,y}$ the beta functions at the interaction point (IP), and finally, σ_x and σ_y the horizontal and vertical rms beam sizes of the opposing beams at the IP, respectively. The parameter ξ roughly corresponds to the linear beam-beam tune shift experienced by a particle at small amplitude. The transverse beam-beam deflection could be shown as that got from the BEPCII luminosity on-line tuning in Fig. 1:

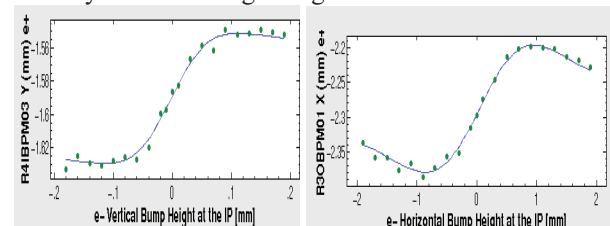


Figure 1: Beam-beam deflection at the BEPCII.

As to the case with crossing-angle at the IP, the bunch length effect due to transverse beam-beam forces could not be neglected when the beams are focused extensively. The transverse kick depends on the longitudinal position as well as on the transverse position. To keep the symplecticity, we should expect, at the same time, an energy change which depends on the transverse coordinates [3].

Large crossing angle at IP can avoid the parasitic collisions when bunch spacing is shortened for more collision bunches in high energy e-e+ colliders. But for large crossing angle, an instability due to synchro-betatron resonances will limit the performance of colliders. The so-called synchro-beam map for a particle-slice interaction, which provides us a 6x6 symplectic map, enables us to install the beam-beam interaction in 6-dimensional weak-strong simulations. Simulation studies show that crossing with a large angle has less serious detrimental effects that is usually believed [4]. The luminosity reduction is only of geometrical, and thus, collision with a crossing angle is popular, such as KEKB, DAFNE and BEPCII, in which horizontal crossing schemes are applied with Piwinski angles of 0.5–1. For a Piwinski angle $\phi \gg 1$, the betatron resonance dominates, but for $\phi < 1$, the synchro-betatron resonance will dominate.

Figure 2 is a 2D tune scanning in the range from 0.5 to 1.0, and also shows the simulation results of for different Piwinski angles. The main resonances could be easily seen.

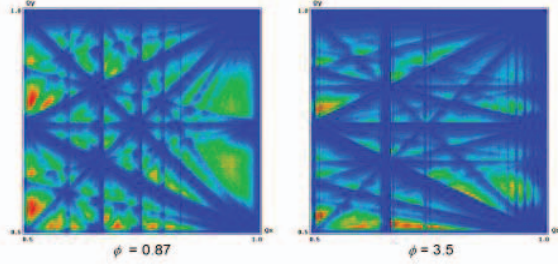


Figure 2: Synchro-betatron (left) and betatron (right) resonances. [Courtesy D. Shatilov, BINP]

Crab crossing is expected to boost the beam-beam parameter and the luminosity as well [5]. Crab cavities were used in KEKB to promote the luminosity about 23% [1], Crab waist scheme was applied in DAFNE [6]. The large Piwinski angle reduces the overlap area near IP, and allows to squeeze the β_y at IP without hourglass effect. The nano scheme, which means an increased Piwinski angle with decreased horizontal beam size and large crossing angle, is adopted in SuperKEKB [7], although new beam-beam resonances were introduced by large Piwinski angle itself.

For a higher energy e-e+ collider, the beamstrahlung, which means synchrotron radiation emits in the strong field of the opposing beam, shown as Fig. 3, becomes a key factor, which has two main effects: (1) energy spread increasing and bunch lengthening due to additional synchrotron radiation with large quantum fluctuation. (2) reduction of the beam lifetime due to the emission of photons of so large an energy that emitting electron, or positron falls outside of the ring. Quantum acceptance and is lost over subsequent turns. It can be described by the self-consistent formula as [8]

$$\sigma_{\delta,tot} = \left(\frac{1}{2} \sigma_{\delta,SR}^2 + \left(\frac{1}{4} \sigma_{\delta,SR}^4 + \frac{1}{4} \frac{\tau_z n_{IP}}{T_{rev}} \sigma_{\delta,BS}^2 \frac{\sigma_{\delta,SR}^2}{\sigma_z^2} \right)^{\frac{1}{2}} \right)^{\frac{1}{2}}, \quad (2)$$

with

$$\sigma_{\delta,BS} \approx \delta_{BS} \left(0.333 + \frac{4.583}{N_\gamma} \right)^{\frac{1}{2}}, \quad \delta_{BS} \approx 0.86 \frac{r_e^3 \gamma N_b^2}{\sigma_z \sigma_x^2}, \quad (3)$$

and

$$N_\gamma \approx 2.1 \frac{\alpha r_e N_b}{\sigma_x}. \quad (4)$$

The momentum acceptance δ_{acc} is not only the static acceptance from the RF system, but given by the off-momentum dynamic aperture. The latter is determined by the off-momentum optical design of the interaction region. The beamstrahlung lifetime is expressed by [9] as

$$\tau_{BS} \approx \frac{1}{n_{IP} f_{rev}} \frac{4\sqrt{\pi}}{3} \sqrt{\frac{\delta_{acc}}{\alpha r_e}} \exp\left(\frac{2}{3} \frac{\delta_{acc} \alpha}{r_e \gamma^2} \frac{\gamma \sigma_x \sigma_z}{\sqrt{2} r_e N_b}\right) \frac{\sqrt{2}}{\sqrt{\pi} \sigma_z \gamma^2} \left(\frac{\gamma \sigma_x \sigma_z}{\sqrt{2} r_e N_b}\right)^{3/2}, \quad (5)$$

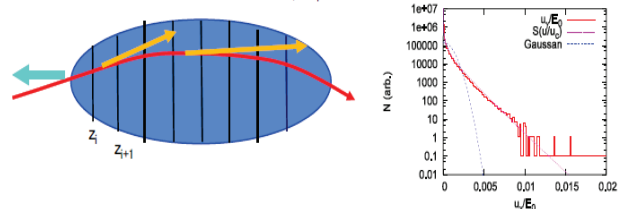


Figure 3: Simulation of beamstrahlung at the IP. [Courtesy K. Ohmi, KEK]

LINEAR LATTICE DESIGN

From the beam-beam simulation, one can find the operation region for high luminosity in a collider. The optics for the arcs in the ring can be chosen as FODO cells as in most of the colliders.

LEP has been successfully operated with $60^\circ/60^\circ$, $90^\circ/60^\circ$, $90^\circ/90^\circ$ and $102^\circ/90^\circ$ phase advances in horizontal and vertical planes per cell, respectively. The choice of phase advance was a key point in LEP's upgrade to higher beam energy. The horizontal beam size naturally increases with beam energy and stronger focusing in the horizontal plane is required to keep the horizontal beam size within manageable limits and to maintain the luminosity performance.

Pretzel scheme and bunch train scheme were both tested in LEP storage ring with maximum 4 equal-distant bunches per beam in the single ring [10]. Electro-static separators were used to make orbit bumps at the parasitic IPs where no detector installed. Figure 4 shows the pretzel orbit and the schematic layout of the bunch train in the LEP storage ring, in which the beams are separated horizontally and vertically around the additional IPs, respectively.

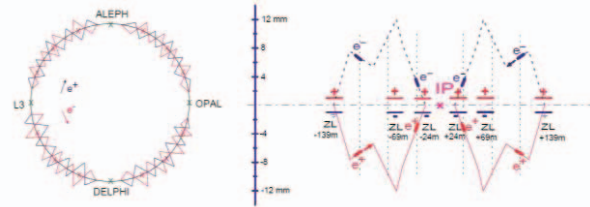


Figure 4: Pretzel orbits and schematic layout (3 bunches per beam) of the bunch trains in LEP storage ring.

Double-ring is used in the FCC-ee lattice design. The arc optics basically consists of $90^\circ/90^\circ$ FODO cells [11]. Two non-interleaved families of sextupole pairs, having a $-I$ transformation between sextupoles, are placed in a 5-FODO superperiod. The number of cell is determined to achieve the equilibrium horizontal emittance, resulting in 292 independent sextupole pairs in a half ring.

The optics of the IR, corresponding to $\beta_{x,y}^* = (1 \text{ m}, 2 \text{ mm})$ is shown in Fig. 5. It has a local chromaticity correction system (LCCS) only in the vertical plane at each side of the IP. Sextupoles are paired at each side, but the inner sextupoles close to the IP have non-zero horizontal dispersion. The outer sextupoles not only cancel the geometrical non-linearity of the inner ones, but also generate crab-waist at the IP by choosing the phase advances between the IP as $\psi_{x,y} = (2\pi, 2.5\pi)$. This incorporation of the crab sextupole

into the LCCS saves space and the number of optical components. Figure 5 gives the Twiss functions of the FCC-ee IR, where the outer ones work as crab sextupoles [11].

Dynamics aperture (DA) is a main concern in the design of colliders, especially the large ring with IR. The DA of FCC-ee has been optimized by searching sextupole settings by particle tracking with the downhill simplex method scripted in SAD.

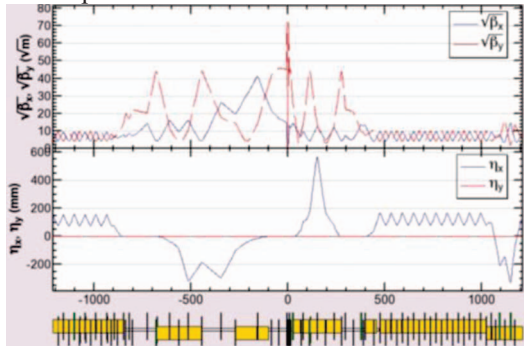


Figure 5: The beam optics of IR for FCC-ee [11].

Figure 6 shows a result of such an optimization. The DA satisfies the requirements for both beam-beam and injection, at least without errors and misalignments, even including the strong-weak beam-beam interactions.

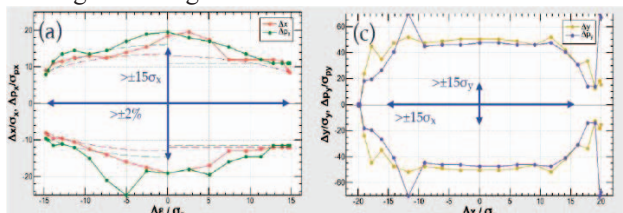


Figure 6: Dynamic apertures after optimization.

The current design of CEPC ring adopts pretzel orbits for multi-bunch collision in a single ring, which can save the budget. A standard FODO cell with 60° phase advance in both transverse planes is applied. One pair of electrostatic separators is used to separate the beams in each arc. The schematic layout of the pretzel orbit and the orbit in one eighth of the ring is shown in Fig.7.

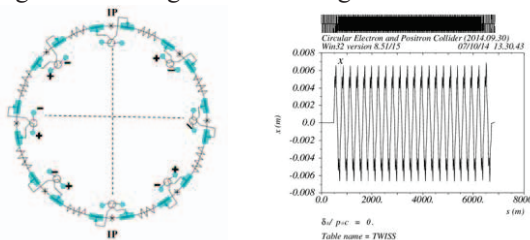


Figure 7: Pretzel scheme used in CEPC single ring (left) and the orbit in one eighth of the ring (right).

Since the beam has an off-center orbit, it will see extra fields in quadrupole and sextupole magnets, which will excite distortions on beam. This can be compensated by tuning the strengths of quadrupoles and sextupoles.

Another option for CEPC ring is a so-called partial double-ring (PDR) scheme, which means some parts of the CEPC ring will be double-ring, as shown in Fig. 8. The detailed design is still in progress. A FODO cell with 90

phase advances in both planes is used in the PDR design, and the full crossing angle of the PDR scheme is 30mrad. More studies on the DA, are still on the way. Figure 9 is the Twiss function of the ring with PDR scheme.

In high energy ring, such as the LEP and LEP2, the beam energy loss per turn due to synchrotron radiation is so large that a kind of energy sawtooth effect has to be considered. The horizontal orbit shift due to the energy sawtooth could be as large as 2.5mm in LEP2 ring, shown as Fig 10.

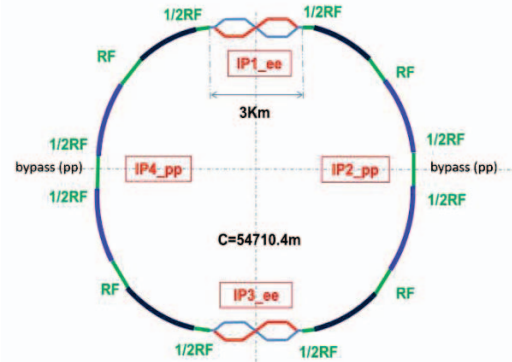


Figure 8: Partial double-ring (PDR) option for CEPC ring.

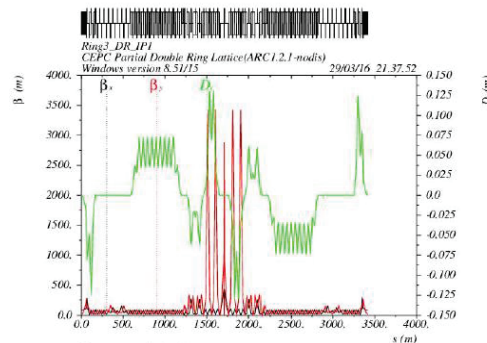


Figure 9: Twiss functions of CEPC PDR scheme.

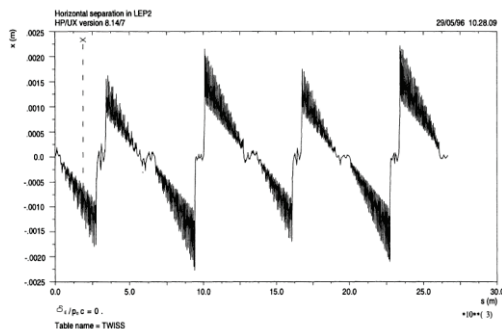


Figure 10: Horizontal positron orbit including sawtooth at 87 GeV of LEP with all RF cavities on.

Energy sawtooth effect at FCC-ee is calculated at the top energy of the beam, i.e., 175 GeV, where the momentum spread due to this effect is as large as 1.1% and the horizontal excursion due to this effect can be as large as 1.8mm [11], which can be seen in Fig. 11. Since the FCC is a double-ring machine, the energy sawtooth can be corrected by magnet strength tapering, i.e., scaling the strengths of all magnets along the local energy of the beam.

Energy sawtooth effect at CEPC had been calculated at Higgs energy, i.e. 120GeV, the momentum spread due to

this effect is about 0.15% and the horizontal excursion due to this effect is about 0.6mm [5], see Fig. 12. This effect at CEPC is shown to have no severe effect on the dynamic aperture [5].

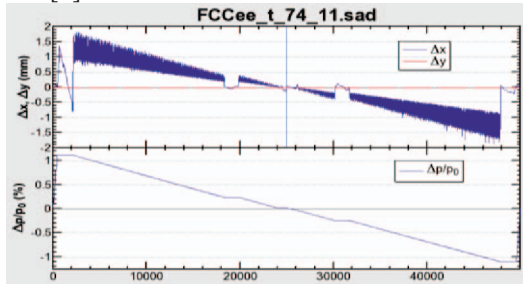


Figure 11: Energy sawtooth in half FCC-ee ring and the beam orbit excursions.

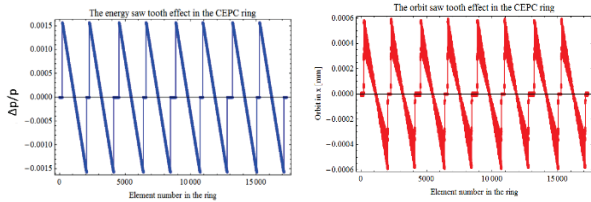


Figure 12: Energy sawtooth in CEPC ring and the resulted beam orbit excursion.

Table 1 lists the main parameters of LEP2, FCC-ee and CEPC [12].

Table 1: Main Parameters of LEP2, FCC-ee and CEPC

	LEP2	FCC-ee (h)	CEPC (pr e-CDR)
Max. E_b (GeV)	104.5	175	120
Circumference (km)	26.7	100	54
Beam current (mA)	4	6.6	16.6
Bunch No. /beam	4	98	50
Particles/beam (10^{11})	23	1.4	3.79
Hori. Emit. (nm-rad)	48	2	6.12
Verti. Emit. (nm-rad)	0.25	0.002	0.018
Bending radius (km)	3.1	11	6.1
Mom. Compact. (10^{-5})	18.5	0.5	3.36
SR power/beam (MW)	11	50	51.7
β_x^* (m)	1.5	1	0.8
β_y^* (mm)	50	1	1.2
$E_{SR}^{loss}/turn$ (GeV)	3.41	7.55	3.1
$V_{rf,tot}$ (GV)	3.64	11	6.87
$\delta_{max,RF}$ (%)	0.77	7.1	5.99
$\delta_{SR,rms}$ (%)	0.22	0.14	0.13
ξ_x/IP	0.025	0.092	0.118
ξ_y/IP	0.065	0.092	0.083
L/IP ($10^{32} \text{cm}^{-2} \text{s}^{-1}$)	1.25	180	204
No. of IPs	4	4	2
Beam lifetime (min)	360	21	47

INTERACTION REGION DESIGN

The IR design of a large collider should follow the following requirements: ensuring small beam sizes at the IP, compensating large chromaticity generated by final doublet locally to achieve as large momentum acceptance as

$\pm 2\%$, compensating the perturbation induced from the detector solenoid, reducing the beam-induced background to detector and fitting the angular acceptance of detector.

A small vertical β at the IP of CEPC is designed to get high luminosity, requiring the final quadrupole to be installed to the IP as close as possible to minimize the chromaticity.

The chromaticity correction scheme of final focus (FF) had been well developed for the linear collider from 1980s, and then adopted by the circular colliders, such as SuperB [13] and SuperKEKB [14]. An FF optics similar to the linear collider is adopted for the CEPC PDR scheme, as a telescopic transfer line including a final telescopic transformer (FTT), chromaticity correction section on the horizontal and vertical planes (CCX and CCY), and the matching telescopic transfer (MT), as shown in Fig. 13 [15]. The L^* , the distance from the IP to the first quadrupole at the IR, is set as 1.5 m for the CEPC, which is an important parameter to the design of detector too.

The dynamic aperture was studied by simulating with the whole ring, but without synchrotron radiation damping. After considering the PDR scheme, we have the results of dynamic aperture of bare lattice at different momentum deviations, shown in Fig. 14 [15], and the optimization results of chromaticity, shown in Fig. 15 [15].

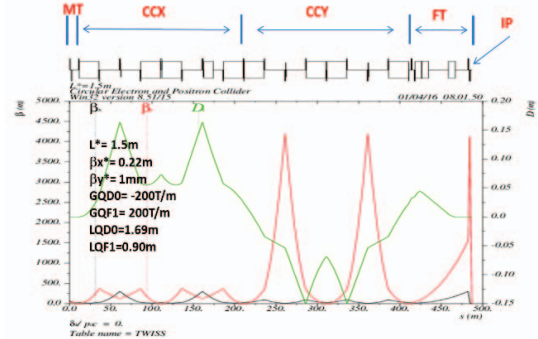


Figure 13: Lattice functions of FF at the CEPC ring.

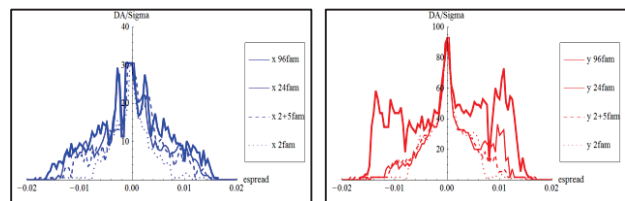


Figure 14: DA results for different sextupole families.

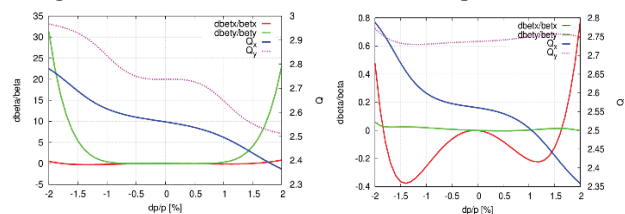


Figure 15: Chromaticities after sextupoles' optimization (left: 1st & 2nd order, right: 3rd order chromaticities).

The 3rd order chromaticity in horizontal plane could be corrected with an additional sextupole at second image point or ARC sextupoles. Much work on dynamic aperture

simulation with SR damping and excitation, magnetic errors, crab sextupoles and solenoid field, is still on the way.

COLLECTIVE EFFECTS

Impedance and collective effects are very critical to factory-like collider. In low energy e+e- collider like BEPCII, impedance is not so easy to be controlled so that the bunch lengthening caused by low frequency impedance dominates the single bunch instability, which cannot be suppressed by feedback system. β_y at the IP was carefully designed with the value similar as the bunch length at the designed bunch current. But in real operation, it is optimized together with the other parameters like transverse emittance coupling, momentum compaction, etc. To get high luminosity, large efforts have been made to increase bunch intensity while decrease bunch lengthening, therefore, collective instability becomes a potential restriction for the machine performance.

In high energy circular e+e- colliders, large bending radius is often chosen due to restricted synchrotron radiation power. Large circumference also means a further enhancement of the machine impedance. Moreover, the large bending radius and small horizontal dispersion in dipoles will generate small momentum compaction factor, which will make the beam more sensitive to collective instabilities.

Microwave Instability

With the well-known Boussard or Keil-Schnell criteria [16, 17], the threshold longitudinal broadband impedance for CEPC is 24 m Ω [18], and for FCC-ee is 13 m Ω [19]. The threshold impedances are considerably low compared to those in B factories, which are in the range of 0.1~1 Ω . Although the analytical criteria is believed to be too passive for short bunched beams, the high frequency part of the impedance may lead to turbulent distributions in longitudinal phase space.

Transverse Beam Tilt

In the transverse plane, when a beam with N particles passes through an impedance with a transverse offset y_b , the tail particles will receive transverse kicks $\Delta y'$, which can be expressed as [20]

$$\Delta y'(z) = \frac{Ne^2}{E_0} \int_0^\infty dz' \rho(z' + z) W_\perp(y_b, z'), \quad (5)$$

where E_0 is the beam energy, ρ the longitudinal distribution, and W_\perp the transverse wake field caused by the beam. This may lead to a transverse displacement of the bunch tail at the interaction point. With the parameters of CEPC, the kick angle along the bunch due to a single RF cavity is shown in Fig. 16.

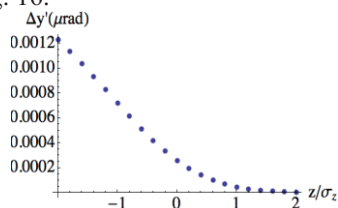


Figure 16: Transverse kick angle along the bunch due to single RF cavity in CEPC ring.

The maximum kick angle at the bunch tail is 1.2 nrad. As there are 384 cavities located in 8 places in the ring, the displacement at IP is 23 nm, which is about one fifth of the beam size at the IP. More detailed simulation studies are under investigation.

Multi-bunch Instability

In high energy e+e- colliders, the revolution frequencies are considerably low, which generate dense beam spectra and is more easily to couple with the narrow-band impedances. One dominant contribution to the coupled bunch instability is the HOMs of the accelerating cavities. To keep the beam stable, the radiation damping time should be less than the rise time of any oscillation mode. In resonant condition, the threshold of shunt impedances are given by

$$\frac{R_L^{th}}{M\Omega} \frac{f_L}{\text{GHz}} < \frac{2(E_0/e)v_s}{N_c I_0 \alpha_p \tau_z} = 16.9, \quad (6)$$

and

$$\frac{R_T^{th}}{M\Omega/m} < \frac{2(E_0/e)}{N_c f_{rev} I_0 \beta_{x,y} \tau_{x,y}} = 17.6, \quad (7)$$

where N_c is the cavity number along the ring, f_L the frequencies of HOMs, f_{rev} the revolution frequency of the ring, E_0 the beam energy, I_0 the beam current, $\tau_{x,y,z}$ the damping time in transverse and longitudinal directions, $\beta_{x,y}$ the transverse beta functions, α_p the momentum compaction, and ν_s the longitudinal tune.

However, considering the whole RF system, one can find that there will be finite tolerances in the cavity construction. The threshold value greatly depends on the actual tolerance of the cavity construction. To avoid RF HOMs, a single mode cavity design is considered for FCC-ee [19].

CONCLUSION

The large circular e+e- collider as a future Higgs factory is of promising as a lot of low energy circular colliders at different energy region have been designed, constructed and operated for many years. In the current design, parameters achieved in previous and current machines make us confident. Despite the contents in this paper, a lot of work such as magnetic error effect to dynamic aperture study, machine-detector interface design including beam induced background control, two stream instabilities, and synchrotron radiation heating problem, need to study carefully and will also determine the performance of future large collider.

ACKNOWLEDGEMENT

The authors is grateful to the efforts given by the team of BEPCII accelerator, and also those who are now working on the CEPC design in IHEP, and those from SLAC, KEK, FNAL, etc.

REFERENCES

- [1] Y. Funakoshi, "Operational experiences on crab cavities in KEKB", ICFA Mini-Workshop on Beam-Beam Effects in Hadron Colliders, 2013.
- [2] D. Berkaev *et al.*, in Proc. of IPAC'11, San Sebastian, Spain, 2011.

- [3] K. Hirata, H. Moshhammer, and F. Ruggiero, *Particle Accelerators*, vol. 40, p. 205, 1993.
- [4] K. Hirata, *Phys. Rev. Lett.*, vol. 74, p. 2228, 1995.
- [5] K. Oide and K. Yokoya, *Phys. Rev. A*, vol. 40, p. 315, 1989.
- [6] M. Zobov *et al.*, *Phys. Rev. Lett.*, vol. 104, p. 174801, 2010.
- [7] <http://www-superkekb.kek.jp>
- [8] K. Ohmi and F. Zimmermann, in *Proc of IPAC'14*, Dresden, Germany, 2014.
- [9] V. Telnov, *Phys. Rev. Lett.*, vol. 110, p. 114801, 2013.
- [10] D. Brandt *et al.*, "Accelerator Physics at LEP", CERN-SL-2000-037 DI, 2000.
- [11] K. Oide, "Design of beam optics for the FCC-ee collider ring", in *Proc. of IPAC'16*, Busan, Korea, 2016.
- [12] H.P. Geng, "Update on pretzel orbit design of CEPC", Internal report, IHEP, 2015.
- [13] Super B Conceptual Design Report, INFN/AE-07/2, SLAC-R-856, LAL 07-15, March 2007.
- [14] Y. Ohnishi *et al.*, Accelerator design at Super KEKB, Prog. Theor. Exp., Phys, 2013, 03A011.
- [15] Y.W. Wang *et al.*, Optimization of CEPC dynamic aperture, CEPC-SppC study group meeting, Beijing, 2016.
- [16] D. Boussard, "Observation of microwave longitudinal instabilities in the CPS", CERN LabII/RF/Int. 75-2, 1975.
- [17] E. Keil and W. Schnell, "Concerning longitudinal stability in the ISR", CERN ISR-TH-RF 69/48, 1969.
- [18] N. Wang *et al.*, "Impedance and collective effects studies in CEPC", HF 2014.
- [19] M. Migliorati *et al.*, "Impedance and collective effects", FCC Week 2015.
- [20] A. Chao and M. Tigner, "Handbook of Accelerator Physics and Engineering", World Scientific 1998.